

# Experimental Study of Quenching Agent on AA6061-Sea Sand Composite: Effect Quenching Medium to Mechanical Properties and Distortion

Tubagus Adytia Syarief Hidayat

Department of Mechanical Engineering, Faculty of Engineering, Universitas Sebelas Maret

Surojo, Eko

Department of Mechanical Engineering, Faculty of Engineering, Universitas Sebelas Maret

Ariawan, Dody

Department of Mechanical Engineering, Faculty of Engineering, Universitas Sebelas Maret

Hammar Ilham Akbar

Department of Mechanical Engineering, Faculty of Engineering, Universitas Sebelas Maret

他

<https://doi.org/10.5109/7236870>

---

出版情報 : Evergreen. 11 (3), pp.2273-2283, 2024-09. 九州大学グリーンテクノロジー研究教育センター

バージョン :

権利関係 : Creative Commons Attribution 4.0 International

# Experimental Study of Quenching Agent on AA6061-Sea Sand Composite: Effect Quenching Medium to Mechanical Properties and Distortion

Tubagus Adytia Syarief Hidayat<sup>1</sup>, Eko Surojo<sup>1,\*</sup>, Dody Ariawan<sup>1</sup>,  
Hammar Ilham Akbar<sup>1,2</sup>, Fahmi Imanullah<sup>1</sup>, Elvira Wahyu Arum Fanani<sup>1</sup>

<sup>1</sup>Department of Mechanical Engineering, Faculty of Engineering, Universitas Sebelas Maret, Surakarta 57126, Indonesia

<sup>2</sup>Department of Mechanical Engineering, Vocational School, Universitas Sebelas Maret, Surakarta 57126, Indonesia

\*Author to whom correspondence should be addressed:

E-mail: esurojo@ft.uns.ac.id

(Received October 31, 2023; Revised February 5, 2024; accepted September 7, 2024).

**Abstract:** The T6 heat treatment is commonly used in manufacturing AMC components. The results of quenching in the presence of oil, water, and brine solution respectively showed an increase in the hardness and tensile strength of the AA6061-Sea sand composite as the cooling rate increased. But on the other hand, the increase in mechanical properties also produces greater distortion as the cooling rate increases. It can be concluded that the faster cooling rate improves the mechanical properties, but also increases the distortion of the AA6061-Sea sand composite.

Keywords: aluminum; composite; heat treatment; quenching

## 1. Introduction

Environmental issues have become a major topic of study in various fields in the last decade. One of the main focuses is on energy saving, especially in the transportation and construction sectors<sup>1</sup>). Several steps have been studied to reduce energy consumption, one of which is the use of lightweight materials in the transportation sector. This encourages the researchers to develop materials that are lightweight but have similar strength to steel. One of the materials being developed is aluminum matrix composite (AMC).

The aluminum matrix composite has massively developed due to its excellent weight-to-strength ratio. In addition, aluminum matrix composites also have a good surface appearance, corrosion resistance, low production costs, and improved mechanical properties<sup>2,3</sup>). These various advantages make aluminum matrix composites widely used as automotive, marine, and aerospace components<sup>3-5</sup>). Several automotive manufacturers use aluminum matrix composites as pistons. Meanwhile, in the aerospace sector, aluminum composites are used as landing gear components<sup>2</sup>). In the military field, the use of aluminum composites is among the manufacturing of bulletproof clothes and military vehicles or fighter aircraft<sup>6</sup>).

Aluminum matrix composites are generally produced

by liquid stage processing<sup>6,7</sup>). Several methods that are often used are squeeze casting, compo casting, and stir casting<sup>2,8-11</sup>). Squeeze casting in general is a process of combining forging and casting. The process begins with metal being melted in a crucible. After melting the metal is stirred and given reinforcing particles. The next process is the process of pouring molten metal into the die which is then carried out by the forging process<sup>12</sup>). Compo casting is the process of making an aluminum matrix composite by first melting the molten metal in a crucible. Once the metal has completely melted, a stirring process can be carried out to produce a material that has a good particle distribution. Aluminum matrix composite which has been completed through the stirring process is then poured into the mold. After the material has cooled, proceed with the hot extrusion semi-solid forming process<sup>12</sup>).

The stir casting process is a composite manufacturing process in which the materials are combined in liquid metal through mechanical stirring and forming vortexes to obtain an even distribution. The stir casting process is suitable for metal matrix composites because of its cost-effectiveness, ease of mass production, and easier control of the composite structure<sup>13-15</sup>). Schematic of the stir casting process consisting of a furnace, crucible, and stirrer impeller. Furnaces are used to heat and melt metals. Crucible is used to place molten metal. The stirrer

produces vortex which are used to mix the reinforcing powder and matrix.

The squeeze casting and compo casting methods have relatively more complex installations and require high costs in the manufacturing process. In addition, the number of products suitable for the squeeze casting and compo casting methods is large-scale. Therefore, stir casting is superior because the installation is more concise and the cost is low, in addition, the amount of production stir casting can be used both on a small and large scale<sup>16)</sup>. Stir casting is a method of manufacturing aluminum matrix composites that utilize vortex flow to induce molten metal dispersion onto reinforcing particles which generally use ceramic particles and oxides such as TiC, B<sub>4</sub>C, Al<sub>2</sub>O<sub>3</sub>, SiC, SiO<sub>2</sub>, Si<sub>3</sub>N<sub>4</sub> and Fe<sub>2</sub>O<sub>3</sub><sup>17,18)</sup>. However, the use of ceramic and oxide particles increases the cost of producing aluminum matrix composites, so researchers switch to using organic materials such as sea sand, red mud, and bamboo leaf ash as reinforcement in aluminum matrix composites. Based on previous studies, sea sand contains SiO<sub>2</sub> and Al<sub>2</sub>O<sub>3</sub> compounds which are capable of providing a reinforcing effect on aluminum matrix composite materials<sup>19)</sup>.

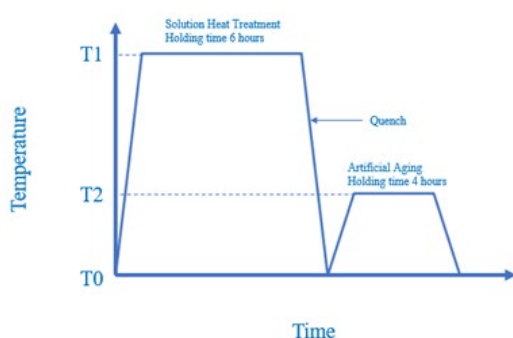


Fig. 1: T6 heat treatment process.

Manufacturing of aluminum matrix composites through the stir casting method produces aluminum composite ingots that have low mechanical properties, so heat treatment is necessary to improve their mechanical properties. The T6 heat treatment is commonly used to improve the mechanical properties of aluminum composites, as shown in Fig. 1. The T6 heat treatment process is divided into three stages, namely: solutioning, quenching, and artificial aging. Quenching is a critical step where the material is cooled rapidly to room temperature. The cooling rate should be done quickly to obtain maximum mechanical properties. But on the other hand, rapid cooling causes thermal shock in the material<sup>20)</sup>. Large temperature gradient changes cause distortion which results in defects in the material<sup>21)</sup>.

Previous studies have shown that quenching using oil, water, and brine media produces the highest mechanical properties in brine quenching media, according to the cooling rate. However, inversely with the distortion that occurs. Quenching with oil and water media shows lower

distortion than quenching with brine<sup>22)</sup>. Rapid cooling using water at room temperature on ZrB<sub>2</sub>-SiC causes crack propagation and deflection in the material<sup>23)</sup>. Buczek et al.<sup>24)</sup> studied quenching with water, oil, and polymer solutions. A quenching process with a lower cooling rate than water results in smaller distortion and larger Mg<sub>2</sub>Si size<sup>24)</sup>. Quenching trials with water media on ceramics have been carried out by Haibo Kou et al. resulting in cracks on the surface of the specimen<sup>25)</sup>.

Zhixin Li et al. conducted research using the quenching spinning method using water cooling media on material AA2219. AA2219 is widely used as a material in the aerospace and aviation industries because it has high mechanical properties and is suitable for structural reliability. The quenching spinning method is used to reduce the distortion that occurs due to the quenching process, so that the shape and size of the product will be more precise. Residual stress that occurs due to the quenching process is also one of the factors that causes the formation of imprecise components. In his research, the quenching spinning method using water media is expected to reduce the residual stresses that arise so that the components can be more precise and according to the desired dimensions<sup>26)</sup>.

A high severity is still needed to extricate heat more quickly. Severity is the ability of the quenching medium to extract heat from the specimen so that the temperature gradient difference can have a strengthening effect on the composite metal. However, in the quenching process, it should be noted that thermal shock due to the cooling rate on the specimen causes distortion and crack initiation<sup>25)</sup>.

Based on previous research, the discussion of aluminum heat treatment is limited to optimizing temperature and holding time for the mechanical properties of aluminum and ceramics. Literature on the effect of the quenching process on optimizing the mechanical properties and distortion of aluminum composites is very limited. The microstructure is observed to validate the phenomena that occur during the quenching process. Microstructural observations are expected to complement the reasons for differences in cooling rates which have an impact on the mechanical properties of the material. It is necessary to pay attention to the existing distortion effects because this composite has the potential to be used in the transportation, automotive and military fields which have high precision standards<sup>27)</sup>. So, this work aims to examine the quenching process with various media and its effect on mechanical properties and distortion of aluminum matrix composites with natural-based reinforcement.

## 2. Materials and method

### 2.1 Aluminum as matrix

Aluminum is one of the metals with various advantages in demand in the automotive and aviation industry. To obtain desired mechanical properties, aluminum can be

combined with other reinforcement particles<sup>28)</sup>. Aluminum is a metal that has the potential to be developed because of its advantages in various aspects, such as lightweight and corrosion resistance<sup>29)</sup>. Pure aluminum has mechanical properties that are below those of metallic materials currently used in the automotive, transportation, and military fields. The researchers then innovated and carried out developments by combining aluminum with reinforcing particles so that it became an aluminum composite material that has mechanical property close to production standards in that field. Therefore, the researchers saw great opportunities and potential in developing materials made from aluminum matrix composites. Aluminum also has different characteristics based on the series the different composition of each aluminum series has different properties.

The Aluminum 6xxx was chosen as a matrix because it has Mg and Si elements needed to improve its mechanical properties. The presence of Si particles can increase strength and formability besides that Mg particles also increase corrosion resistance but reduce strength. In addition, it takes a high strength but has lightweight, coupled with good formability, welding ability, resistance to wear and corrosion, and low costs making it a material that has great potential in developing strong but lightweight materials<sup>1)</sup>.

Aluminum 6061 was chosen to be a matrix material that will be combined with reinforcing particles because it has advantages in the industry when compared to other series<sup>30)</sup>. Aluminum 6061 is commonly used as a matrix because of the versatility between other series and is mostly produced using the casting stir method.

## 2.2 Sea sand as reinforcement

The addition of reinforcing particles in the stir-casting process aims to improve mechanical properties. Generally, the reinforcing particles used are ceramic particles such as  $\text{Al}_2\text{O}_3$ ,  $\text{SiC}$ , and  $\text{TiO}_2$ <sup>28,31)</sup>. Ceramic particles are hard and have a high melting point. Some researchers add these ceramic particles to aluminum to improve its mechanical properties. Ceramic particles that have been widely used have a relatively expensive price which is a limitation for researchers to explore. This is what underlies some researchers then look for alternative reinforcement particles such as agro-waste and also sea sand<sup>32)</sup>. Both agro-waste and sea sand are economical alternatives for reinforcing particles. Both are known to contain ceramics so they can be used as composite reinforcing particles.

Sea sand was chosen as an alternative to strengthen the matrix because it contains ceramic particles and in terms of economical production cost. The size, content, and shape of sea sand particles have been studied because it affects the physical and mechanical properties of composite<sup>33)</sup>. Sharanova et al.<sup>34)</sup> found the physical properties of sea sand from Yantarny, the Kaliningrad region, Russia, and confirmed that the actual density of sea sand and bulk was  $2612 \text{ kg/m}^3$  and  $1474 \text{ kg/m}^3$ . Iron

sand investigation from Syiah Kuala Beach, Banda Aceh, Indonesia, revealed that Magnetite ( $\text{Fe}_3\text{O}_4$ ) is the dominant phase with 85%, with a minor phase including  $\text{TiO}_2$ ,  $\text{SiO}_2$ ,  $\text{Al}_2\text{O}_3$ <sup>35)</sup>. Akbar et al.<sup>10)</sup> produces AMC using sea sand as a reinforcement. Sea sand used is obtained from Samas, Yogyakarta, Indonesia, and the result is that sea sand can be mixed with liquid aluminum using a complaint process.

The XRD test of previous studies is shown in Fig. 2. Figure 2 revealed that sea sand compositions such as diopside (38,9%),  $\text{SiO}_2$  (42,2%),  $\text{Fe}_2\text{MgO}_4$  (14,1%), and  $\text{Fe}_3\text{O}_4$  (4,7%) which have higher hardness when compared to aluminum. The XRD of sea sand also shows properties such as density of  $2.5 \text{ g/cm}^3$ , modulus of elasticity 124.28 (GPa), and hardness 6-6.5 (Mohs).  $\text{SiO}_2$  in sea sand has a density of  $2.65 \text{ g/cm}^3$  and a melting point of around  $1600^\circ\text{C}$ . The  $\text{Fe}_3\text{O}_4$  contained has a density of  $5 \text{ g/cm}^3$  and a melting point of around  $1550^\circ\text{C}$ . This study uses 150 mesh sea sand, so that the grain size is between  $1\text{-}100 \mu\text{m}$ . The shape of the sea sand has shown in Fig. 3.

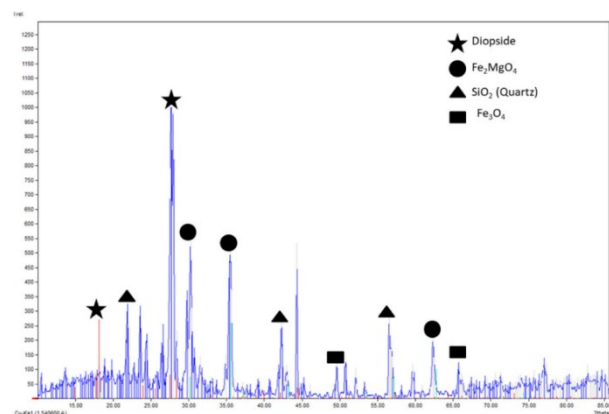


Fig. 2: Results sea sand XRD<sup>19)</sup>.

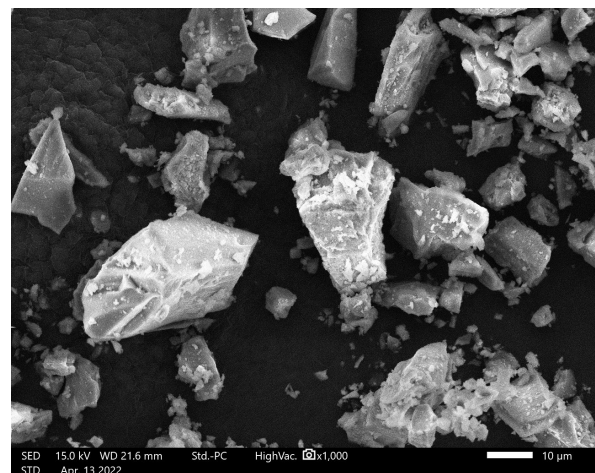


Fig. 3: Microstructure of sea sand.

## 2.3 Composite manufacturing

The composites were produced by the stir casting method using the apparatus shown in Fig. 4. By reviewing the research that has been done by other researchers related to AMC fabrication, the stir casting method was

chosen because combining aluminum with reinforcing particles will be easier. This method has the advantages of low cost, can produce larger, and easy installation. However, in fact, this method has a weakness in the wettability factor. Wettability is the ability of the reinforcing particles to unite with the matrix used, in this case, aluminum. The addition of Mg as a wettability enhancer has also been researched by Rahman et al.<sup>36</sup>. Researchers found that the effect of Mg during the stir-casting process can increase wettability so that the bonds between particles will be stronger.

The process of making the composite: the first step, 150 mesh of sea sand is washed using alcohol to eliminate the impurities. Then melt the aluminum matrix smelting process using a graphite crucible at 720-740°C. The stirring process uses the four impeller blades at an angle of 45° with a diameter of 50 mm made from SS 304 with TiO<sub>2</sub> coated. After that, sea sand particles (4% wt) were added to the molten aluminum. The stirring process was carried out for 10 minutes with a stirring speed of 600 rpm. Then the molten composite was poured into a permanent steel mold with dimensions of 130 x 130 x 60 mm and heated before at a temperature of 500°C. After the specimen is removed from the mold, the machinery process is followed to be adjusted to the dimensions of tensile, hardness, and distortion tests.

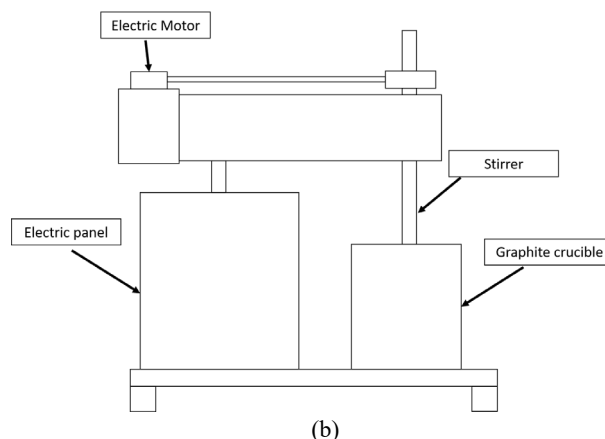
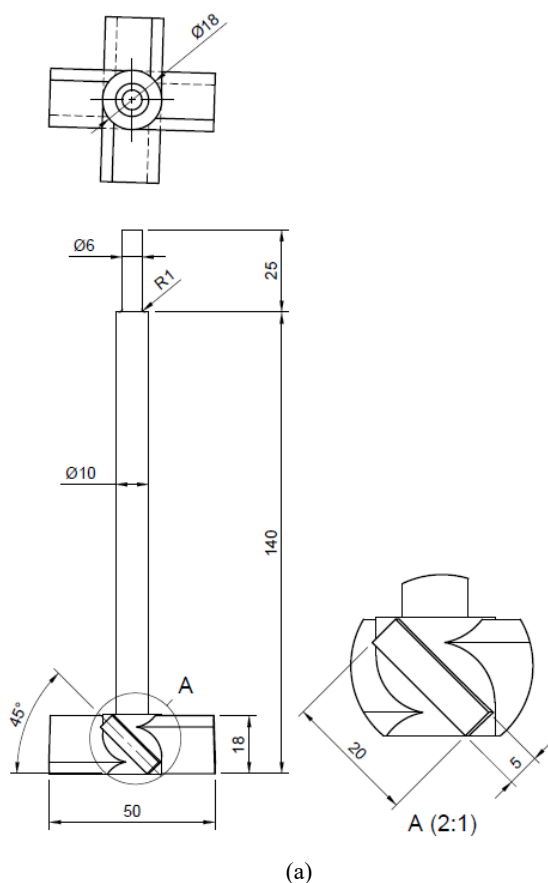


Fig. 4: a) Impeller coated with TiO<sub>2</sub>, b) Stir casting apparatus.

The specimen codification without heat treatment is Non-Treatment Specimen (NT), the second specimen uses oil as quenching media (TO), the third specimen uses water as quenching media (TW) media, and the last specimen uses brine (salt solution) as quenching media (TB). Specimens have been treated under T6 heat treatment. The solution heat treatment has been carried out for 6 hours at 540°C. Then the specimens were rapidly cooled in various quenchants (water, oil, brine) and followed by artificial aging treatment for 4 hours at a temperature of 200°C.

Table 1. Notation specimen quenching media.

Notation	Treatment
NT	Non-Treatment
TO	Treatment oil quenching media
TW	Treatment water quenching media
TB	Treatment brine quenching media (salt solution 10%)

Table 1 shows the notation set for each specimen category. NT (non-treatment) notation shows that the T6 heat treatment process is not carried out after the specimen is taken from the mold.

## 2.4 Testing method

### 2.4.1 Tensile test

The tensile strength was tested using the Servo Hydraulic Universal Testing Machine (Sans Testing Machinery., Ltd., Shenzhen, Guangdong, China). The tensile test was carried out according to JIS Z 2201<sup>37</sup>, with a tensile speed of 10 mm/minute. The tensile test dimension specimen is shown in Fig. 5.

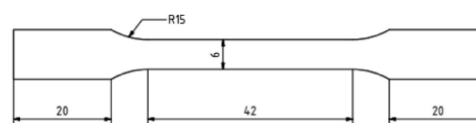


Fig. 5: Specimens tensile test AA6061-Sea sand.



The tensile test is done by applying the tensile load to the specimen at the specified speed until the specimen is a fracture. The load is recorded by the load cell and then processed so that the tensile graph is obtained. The test results can be used to calculate the tensile stress using Equation 1.

$$\sigma = \frac{F}{A_0} \quad (1)$$

The stress is obtained by applying the load given perpendicular to the specimen cross-section. strain and modulus elasticity can be calculated from the strain-stress curve that allows the characteristics of the material tested to be identified. The strain of the specimens has been calculated strain Equation 2.

$$\varepsilon = \frac{l_1 - l_0}{l_0} \quad (2)$$

The strain is calculated from the length of length when the specimen tested. The stress is directly proportional to the strains in the elastic area. The modulus of elasticity of the material was calculated by the stress curve, which allows the material to be classified as ductile or brittle.

#### 2.4.2 Hardness test

Composite hardness was measured using O.M.A.G Affri Italy Mod 100 MR (PreviTi, Lecco, Italia) according to ASTM E-10<sup>38)</sup>, with 5 mm steel ball indenter and 125 kgf load. The Brinell hardness of the composite is determined using Equation 3, where P is the applied load, D is the diameter of the indenter, and d is the width of the indentation in the specimen. The hardness obtained is the average value of nine indentations with a time of 30 seconds at each loading which is ed in the Brinell Hardness Number (BHN).

$$BHN = \frac{2P}{(\pi D)(D - \sqrt{D^2 - d^2})} \quad (3)$$

Hardness testing is carried out by emphasizing the surface of the specimen with steel ball indenters and time according to the standard, which will cause indentation on the surface of the specimen. This test is used to determine how well the specimen can withstand deformation. The results of this test are also used to determine whether the material to be used meets the quality standards of each industry. The purpose of hardness testing in this case is to examine materials made of pure metal or alloy metal. Effects caused by manufacturing processes such as pressure, loading, and thermal effects will affect the quality of the material.

#### 2.4.3 Distortion test

The distortion test used in this study was Coordinate Measuring Machine (Mitutoyo Strato Bright 707, Kanagawa, Japan). The test is carried out by measuring

the surface of the composite AA6061-Sea sand in different conditions. The distortion results are obtained from the difference in measurements before and after heat treatment.

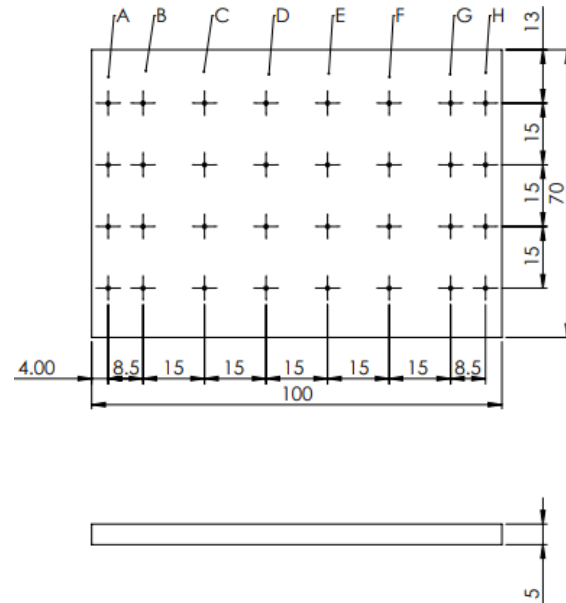


Fig. 6: Coordinate position CMM test (in mm).

Figure 6 showed the dimensions of the specimen and the position of the test point. The test point is denoted from A to H. The 32 test point serves as a reference for the distortion. Test point A is 4 mm from the end of the specimen, and the distance from A and B is 8.5 mm. Point B to C is 15 mm. This test point was chosen to see the effect of the cooling rate on the specimen dimension. It also aims to show that the cooling rate causes large distortion, especially on the edge of the specimen.

#### 2.4.4 Microstructure observation

Microstructure observation was carried out to determine the grain shape and grain size of the aluminum matrix before and after heat treatment. Microstructure observation was carried out using optical microscope devices produced by Euromex Holland, Arnhem, Netherlands.

The etching solution used was Keller's Reagent with the composition of 2 ml of HF, 3 ml of HCl, 5 ml of HNO<sub>3</sub>, and 190 ml of distilled water.

### 3. Results and discussion

#### 3.1 Tensile test and hardness test

The tensile strength and hardness of the AA6061-Sea sand composite are shown in Fig. 7 and Fig. 8, respectively. Gireesh, et al's research was used as a benchmark for the mechanical strength of the AA6061-Pure obtained a hardness value of 30 HBN and a tensile force of 115 MPa<sup>39)</sup>. The tensile strength and hardness of the composite increased after the heat treatment. The

increase in strength and hardness resulting from heat treatment was influenced by the quenching media used. The tensile strength of the composites using quenching media of brine, water, and oil was 208.23 MPa, 198.18 MPa, and 188.35 MPa, respectively. A similar phenomenon also occurs in the AA6061-Sea sand composite hardness test. The hardness of the composites using quenching media of brine, water, and oil was 59.36 BHN, 55.76 BHN, and 51.55 BHN, respectively.

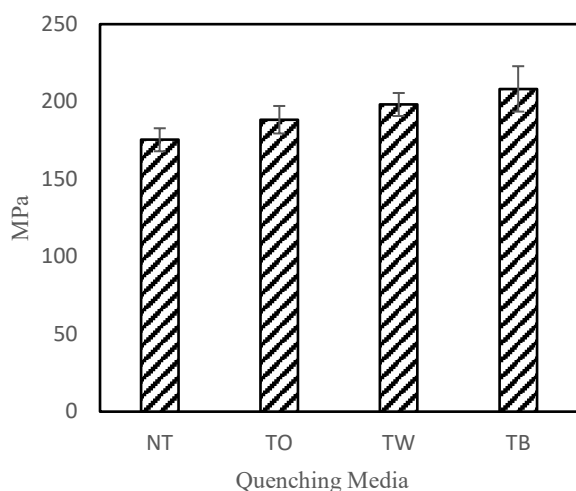


Fig. 7: Ultimate tensile strength composite AA6061-Sea sand.

Table 2. Mechanical properties AA6061-Sea sand.

Notation	Non-Heat Treatment	Water	Brine	Oil
Ultimate Tensile Strength (MPa)	175.42	198.18	208.23	188.35
Elongation (%)	6	4.64	2.8	5.36
Elastic Modulus (MPa)	1835.55	2960.69	3368.58	1954.85

Table 2 presents the ultimate tensile strength, elongation, and elastic modulus of each specimen with different quenching media. Tensile strength is always inversely related to elongation, this shows that the stronger material will produce a more brittle material<sup>40)</sup>. Elastic modulus is also inversely related to elongation. A material that has a high elastic modulus indicates that the material is getting stiffer (brittle)<sup>41)</sup>. Ultimate tensile strength is always inversely proportional to elongation, so it is necessary to examine which treatment is appropriate in each case.

The modulus of elasticity and strain will decrease because after rapid cooling the material will change its properties to become more brittle compared to before<sup>22)</sup>. The modulus of elasticity of each variation shows varied

results, this is influenced by the cooling rate of each different quenching media. The rapid cooling rate causes more precipitate compounds to be trapped in the grain. The increasing mechanical strength of a material will reduce the strain which causes the value of the modulus of elasticity to vary. Cooling rates that are too fast also cause high residual stress. This occurs because, during the solution heat treatment conditions, the material is forced to cool by immersing it in the quenching medium<sup>42)</sup>. Quenching media have different levels of heat extractions, by looking at this phenomenon, when the dyeing process occurs the material will experience residual stresses that occur due to the large temperature gradient in the aluminum matrix composite<sup>43)</sup>. The cooling rate affects the improvement of mechanical properties when looking at the phenomenon that occurs during quenching treatment.

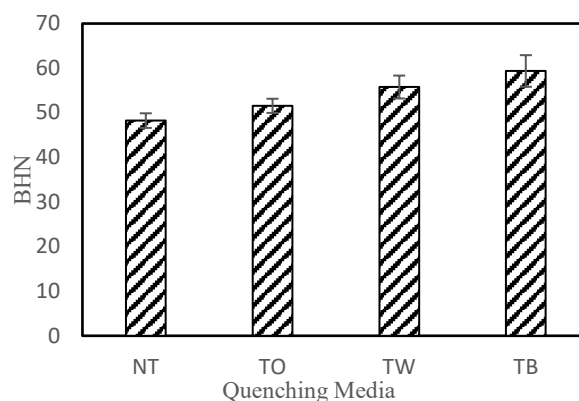


Fig. 8: Hardness of the composite AA6061-Sea sand.

The mechanical properties test showed that the lower the cooling rate, the lower the resulting mechanical properties. This is in line with the cooling rate of each cooling medium. The cooling rate of the cooling medium is related to its severity (H). Brine solution has an H coefficient of 2.0-2.2 while water and oil have an H coefficient of 1.0-1.1 and 0.30-0.35<sup>22)</sup>. The cooling rate also affects the growth of the  $Mg_2Si$  precipitation compound which affects the mechanical properties of the composite<sup>44)</sup>. In addition to affecting the precipitate compounds, extreme temperature gradient changes result in a slip in the aluminum matrix. This irregularity also increases the mechanical properties of the composite<sup>45)</sup>.

Each quenching medium has a different character. This is due to the cooling rate. The cooling rate shows the phase transition that occurs when the aluminum composite is immersed in a different medium. During the formation phase of primary precipitation, latent heat is extracted so that the temperature drop is rapid. The second precipitate phase also undergoes heat extraction but in small amounts, so that when there is a rapid decrease in heat, many of the precipitate phases are trapped in the grains. This is what causes mechanical properties to increase because the trapped phases such as  $Mg_2Si$  function as obstacles to the

movement of dislocations<sup>40)</sup>.

The speed of the cooling rate also determines the elements spread phase that occurs. The slow cooling rate causes the size of  $Mg_2Si$  to increase so that it will reduce mechanical properties<sup>43)</sup>. This is what causes the difference in the formation of precipitate in the AA6061-Sea sand composite. The Mg and Si elements which are spread evenly and trapped are what causes the increase in mechanical properties. The cooling rate also inhibits the growth of  $Mg_2Si$  at grain boundaries. At grain boundaries where there is a lot of  $Mg_2Si$  will reduce the bond strength between grains<sup>46)</sup>.

The slow cooling rate also causes the Si particles to cluster in one location, as it is known that Si particles have low solubility in aluminum. The accumulation of Si due to the low cooling rate makes the grain larger. On the other hand, rapid cooling rate will induce a smaller dispersion density and enable nanoscale precipitation of precipitates. The fast cooling rate can also cause the effect of increasing the bond between the matrix and the reinforcing particles because the low temperature can make the  $Mg_2Si$  intermetallic phase more stable to the matrix<sup>47)</sup>.

### 3.2 Distortion test

Distortion is a deviation or change in shape and dimensions caused by heat. Distortion is something to avoid, especially in automotive applications. If the material is distorted it will cause its dimensions to change which will affect the precision. Distortion testing is shown in Fig. 9.

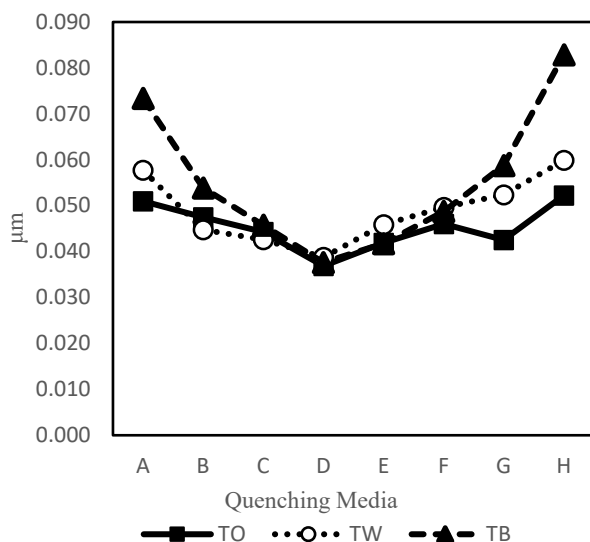


Fig. 9: Distortion tendency of the composite AA6061-Sea sand.

The quenching process using brine solution produces the biggest distortion compared to the quenching process with other media. Brine has the highest cooling rate reaching  $2300^{\circ}C/s$  compared to water and oil is  $150^{\circ}C/s$  and  $90-110^{\circ}C/s$ <sup>48)</sup>. High cooling rates will produce

distortion. Distortion occurs due to the rapid cooling process at the quenching stage, generally, the biggest distortion occurs at the edge of the specimen<sup>49)</sup>. The amount of distortion that occurs depends on several factors, including the cooling rate, the geometry of the object and the temperature of the cooling medium<sup>25,50)</sup>. Rapid cooling creates residual stresses that initiate distortion and cracks, residual stresses arise as a result of large temperature gradient changes in the material, especially on its surface<sup>51,52)</sup>.

Table 3. Distortion value of 3 media quenching.

Measuring point	Brine	Water	Oil
	Average 4-point measuring		
A	0,073	0,058	0,051
B	0,054	0,045	0,048
C	0,046	0,043	0,044
D	0,038	0,039	0,037
E	0,042	0,046	0,042
F	0,049	0,05	0,046
G	0,059	0,052	0,043
H	0,083	0,06	0,052

In Table 3 it can be seen that the largest distortion values occur at points A and H which are on the edge of the specimen. The distortion point is obtained by analyzing the changes in the surface coordinates of the specimen before the T6 heat treatment and after the T6 heat treatment. The above data is the average distortion that occurs at each test point on the surface of the specimen. The smallest distortion is in the middle of the specimen, namely at points D and E. This is because the greatest thermal expansion occurs at the edge of the specimen resulting in a very large temperature gradient difference.

Specimens with slow cooling rates show the smallest distortion, while fast cooling rates show the biggest distortion changes. In slow cooling, the distortion that occurs is small because the heat extraction of the media requires a longer time compared to the brine media, which has a greater severity. On rapid cooling, even the atoms do not have time to rearrange the position of the crystal structure and finally, an amorphous precipitate is formed<sup>25)</sup>.

The difference in the coefficient of thermal expansion or the ability to release heat from the reinforcing particles and the aluminum matrix results in an inconsistency of thermal stresses<sup>24)</sup>. It is this different coefficient of thermal expansion that distorts due to the fast cooling rate<sup>47)</sup>. If we compare the data from the distortion test results with the data from the mechanical test results, there is the same trend. The harder a material is, the more unstable the dimensions will be due to the quenching process<sup>53)</sup>.

So the cooling rate needs to be done as fast as possible, but the effects caused in the form of distortion also need to be considered<sup>53)</sup>. The cooling rate also reduces the optimal value that can be achieved by the material. The



thermal stress that causes some of these negative impacts needs to be considered<sup>54</sup>, because its application in automotive, transportation, and military will greatly affect the durability and precision of the product.

### 3.3 Microstructure investigation

The following is a picture of the microstructure of each specimen.

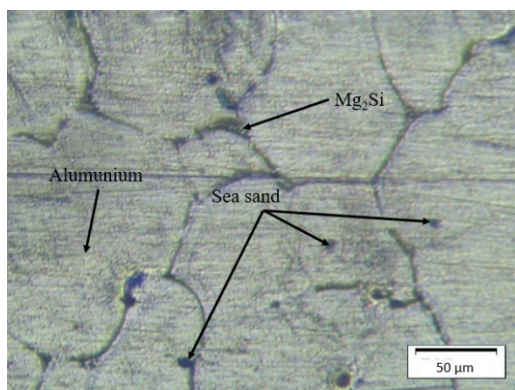
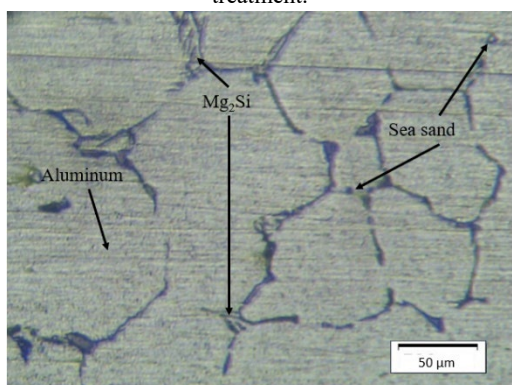
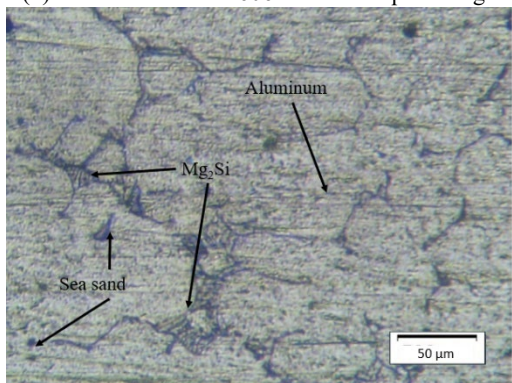


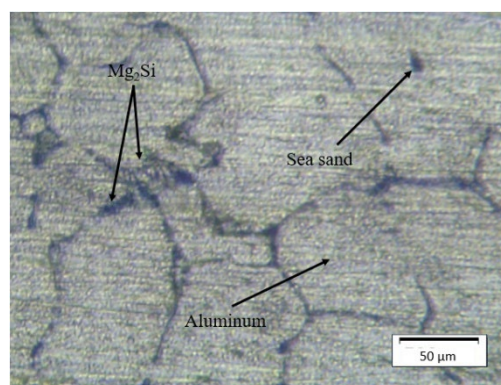
**Fig. 10:** (a) Microstructure AA6061-Seal sand without treatment.



(b) Microstructure AA6061-Seal sand quenching oil.



(c) Microstructure AA6061-Seal sand quenching water.



(d) Microstructure AA6061-Seal sand quenching brine 10%.

The method used to identify the presence of  $Mg_2Si$  in this study is the observation of metallographic structure using optical microscopes. The processes carried out include sander and polish on the sample, followed by the etching process using a Keller reagent solution. Figure 10. (a) shows the Microstructure of AA6061-Seal sand without treatment. It can be seen that the sea sand distribution is evenly distributed on the surface. An even distribution indicates that the reinforcing material is mixed optimally. Figure 10. (b) shows the Microstructure of AA6061-Seal sand quenching oil. When compared with Fig. 10. (a) Microstructure AA6061-Seal sand without treatment at grain boundaries showed more  $Mg_2Si$ . This is due to the slower cooling rate of the oil medium, allowing  $Mg_2Si$  to grow at the grain boundaries. The AA6061-Seal sand quenching water microstructure is shown in Fig. 10. (c). The grain size when compared to Microstructure AA6061-Seal sand without treatment is finer and there are lots of  $Mg$  and  $Si$  particles in the grains. The microstructure of AA6061-Seal sand quenching brine 10% is shown in Fig. 10. (d). When compared to the microstructure of other specimens, the grain size is finer, and more  $Mg_2Si$  are trapped in the middle of the grains. Overgrowth of  $Mg_2Si$  at the grain boundaries causes the mechanical properties to decrease. This is in accordance with the data shown in Fig. 7. and Fig. 8.

The cooling rate affects the microstructure as written in the paragraph above by comparing Fig. 10. (a) Microstructure AA6061-Seal sand without treatment as a reference, the cooling rate makes  $Mg_2Si$  trapped in nano-sized grains. The slow cooling rate causes the presence of large  $Mg_2Si$  sizes at grain boundaries, this will weaken the bonds between grains which have an impact on decreasing mechanical properties<sup>40</sup>.

Figure 10 shows a significant difference, namely from the size of the precipitate, this also has an impact on the corrosion resistance of a material in extreme environmental conditions. The reason is the uneven distribution of  $Mg_2Si$ <sup>40</sup>. With the information obtained from the existing literature and microstructure, it can be analyzed that a fast cooling rate is necessary to improve the mechanical properties of the material, with a fast cooling rate it can avoid softer areas so that the material is

not easily damaged and degraded in a corrosive environment<sup>40)</sup>.

The microstructure obtained from the heat treatment of T6 with different cooling media resulted in the fact that the cooling rate affected the distribution of Mg and Si particles. Mg and Si particles here have an important role in the properties of a material. If the Mg<sub>2</sub>Si compound is in the middle of the grains it will improve the mechanical properties of the material because it will detain the movement of the grains. Conversely, if Mg<sub>2</sub>Si are at the grain edges or grain boundaries the material will tend to have lower mechanical properties<sup>49)</sup>.

#### 4. Conclusion

The increase in mechanical properties is always in line with the decrease in the elongation of the AA6061-sea sand composite specimens, this is due to the different characteristics of the aluminum and the reinforcing particles. Tensile and hardness tests showed that the effect of beach sand as reinforcing particles in collaboration with T6 heat treatment could improve mechanical properties. Distortion data also indicates the same thing, with rapidly cooling rate, the dimensions of the specimen will also change. Thermal shock during quenching also needs to be considered as a negative effect because the rapid cooling rate causes residual stresses and crack initiation in the specimen.

It is this relationship between mechanical properties, distortion, and microstructure that underlies AA6061-Sea sand as an alternative material as a step in developing strong and lightweight materials. The collaboration between the reinforcing particles and the heat treatment applied to the composite fabrication has provided a significant improvement effect. Therefore, the development will continue to be carried out to obtain optimal material properties.

In this study, quenching was carried out using oil, water, and brine solutions to determine the mechanical characteristics and distortion of the AA6061-Sea sand composite. The highest tensile strength and hardness of the AA6061-Sea sand composite were obtained by quenching with brine, water, and oil solutions respectively. Cooling rate affects the increase in mechanical properties besides that the distortion also increases. successively values for increasing mechanical properties and distortion are salt, water and oil quenching media. This is due to the cooling rate of each quenching media. The data obtained can be a reference for further research.

#### Acknowledgements

This work was funded by The Ministry of Education, Culture, Research, and Technology of the Republic of Indonesia under the scheme 'Penelitian Tesis Magister (PTM)' with research grant number: 673.1/UN27.22/PT.01.03/2022.

#### Nomenclature

$\sigma$	Stress (MPa)
$F$	Force (kg)
$A_0$	Section Area (mm <sup>2</sup> )
$\varepsilon$	Strain
$l_1$	Length after any load is applied
$l_0$	Length before any load is applied
$BHN$	Brinell hardness number
$P$	test force (Kgf)
$\pi$	phi
$D$	diameter of the ball (mm)
$d$	mean diameter of the indentation (mm)

#### References

- 1) A.S. Baskoro, M.A. Amat, R.D. Putra, A. Widyianto, and Y. Abrara, "Investigation of temperature history, porosity and fracture mode on aal100 using the controlled intermittent wire feeder method," *Evergreen*, **7** (1) 86–91 (2020). doi:10.5109/2740953.
- 2) E.W.A. Fanani, E. Surojo, A.R. Prabowo, and H.I. Akbar, "Recent progress in hybrid aluminum composite: manufacturing and application," *Metals (Basel)*, **11** (12) (2021). doi:10.3390/met11121919.
- 3) D. Kumar, S. Singh, and S. Angra, "Morphology and corrosion behavior of stir-cast al6061-ceo \_ 2 nanocomposite immersed in nacl and h \_ 2so \_ 4 solutions," *Evergreen*, **10** (1) 94–104 (2023). doi:10.5109/6781054
- 4) N. Singh, and R.M. Belokar, "Tribological behavior of aluminum and magnesium-based hybrid metal matrix composites: a state-of-art review," *Mater. Today Proc.*, **44** 460–466 (2021). doi:10.1016/j.matpr.2020.09.757.
- 5) B.. Raveendra, R. S.; Krupakara, P. V.; Prashanth, P. A.; Prashanth, "Enhanced mechanical properties of al-6061 metal matrix composites reinforced with  $\alpha$  -," *J. Mater. Sci. Surf. Eng.*, **4**(7) (December) 483–487 (2016).
- 6) M. Miqdad, and A.Z. Syahril, "Effect of nano al2o3 addition and t6 heat treatment on characteristics of aa 7075 / al2o3 composite fabricated by squeeze casting method for ballistic application," *Evergreen*, **9** (2) 531–537 (2022). doi:10.5109/4794184.
- 7) J. Singh, and A. Chauhan, "Fabrication characteristics and tensile strength of novel al2024/sic/red mud composites processed via stir casting route," *Trans. Nonferrous Met. Soc. China (English Ed.)*, **27** (12) 2573–2586 (2017). doi:10.1016/S1003-6326(17)60285-1.
- 8) R. Tiwari, H. Herman, S. Sampath, and B. Gudmundsson, "Plasma spray consolidation of high temperature composites," *Mater. Sci. Eng. A*, **144** (1–

- 2) 127–131 (1991). doi:10.1016/0921-5093(91)90217-B.
- 9) I. Sahin, and A.A. Eker, “Analysis of microstructures and mechanical properties of particle reinforced alsi7mg2 matrix composite materials,” *J. Mater. Eng. Perform.*, **20** (6) 1090–1096 (2011). doi:10.1007/s11665-010-9738-6.
- 10) H.I. Akbar, E. Surojo, and D. Ariawan, “Effect of Sea Sand Content on Hardness of Novel Aluminium Metal Matrix Composite AA6061/Sea Sand,” in: *Lect. Notes Mech. Eng.*, Springer Singapore, 2020: pp. 307–315. doi:10.1007/978-981-15-4481-1\_31.
- 11) M. Maurya, N.K. Maurya, and V. Bajpai, “Effect of sic reinforced particle parameters in the development of aluminium based metal matrix composite,” *Evergreen*, **6** (3) 200–206 (2019). doi:10.5109/2349295.
- 12) A. Ramanathan, P.K. Krishnan, and R. Muraliraja, “A review on the production of metal matrix composites through stir casting – furnace design, properties, challenges, and research opportunities,” *J. Manuf. Process.*, **42** (September 2018) 213–245 (2019). doi:10.1016/j.jmapro.2019.04.017.
- 13) M.K. Sahu, and R.K. Sahu, “Fabrication of aluminum matrix composites by stir casting technique and stirring process parameters optimization,” *Adv. Cast. Technol.*, (May) (2018). doi:10.5772/intechopen.73485.
- 14) S.P. Dwivedi, T.K. Gupta, and A. Saxena, “An investigation on the mechanical properties of fsp processed silicon nitride reinforced aluminum composite,” *Evergreen*, **10** (3) 1330–1340 (2023). doi:10.5109/7151680.
- 15) Y. Adityawardhana, A.Z. Syahrial, and B. Adjiantoro, “Characteristic of aa 7075-reinforced nano-sic composites produced by stir-squeeze casting and open die cold forging as an armor material candidate,” *Evergreen*, **10** (2) 722–730 (2023). doi:10.5109/6792821.
- 16) D. Das, C. Samal, A.K. Chaubey, and R.K. Nayak, “Influence of thermal treatment and reinforcement content on properties of aluminium matrix composites: a case study,” *Mater. Today Proc.*, **18** 3262–3267 (2019). doi:10.1016/j.matpr.2019.07.202.
- 17) K.K. Alaneme, I.B. Akintunde, P.A. Olubambi, and T.M. Adewale, “Fabrication characteristics and mechanical behaviour of rice husk ash - alumina reinforced al-mg-si alloy matrix hybrid composites,” *J. Mater. Res. Technol.*, **2** (1) 60–67 (2013). doi:10.1016/j.jmrt.2013.03.012.
- 18) J. Kumaraswamy, K.C. Anil, T.R. Veena, G. Purushotham, and K. Sunil Kumar, “Investigating the mechanical properties of al 7075 alloy for automotive applications: synthesis and analysis,” *Evergreen*, **10** (3) 1286–1295 (2023). doi:10.5109/7151674.
- 19) H.I. Akbar, E. Surojo, D. Ariawan, A.R. Prabowo, and F. Imanullah, “Fabrication of aa6061-sea sand composite and analysis of its properties,” *Heliyon*, **7** (8) e07770 (2021). doi:10.1016/j.heliyon.2021.e07770.
- 20) K.C. Nayak, A.K. Pandey, and P.P. Date, “Mechanical and physical characterization of powder metallurgy based aluminium metal matrix hybrid composite,” *Mater. Today Proc.*, **33** 5408–5413 (2020). doi:10.1016/j.matpr.2020.03.134.
- 21) T.L. Fu, Z.D. Wang, Y. Li, J.D. Li, and G.D. Wang, “The influential factor studies on the cooling rate of roller quenching for ultra heavy plate,” *Appl. Therm. Eng.*, **70** (1) 800–807 (2014). doi:10.1016/j.applthermaleng.2014.05.083.
- 22) H.I. Akbar, E. Surojo, D. Ariawan, and A.R. Prabowo, “Experimental study of quenching agents on al6061–al2o3 composite: effects of quenching treatment to microstructure and hardness characteristics,” *Results Eng.*, **6** (February) 100105 (2020). doi:10.1016/j.rineng.2020.100105.
- 23) X. Jin, L. Dong, Q. Li, H. Tang, N. Li, and Q. Qu, “Thermal shock cracking of porous zrb2-sic ceramics,” *Ceram. Int.*, **42** (11) 13309–13313 (2016). doi:10.1016/j.ceramint.2016.05.040.
- 24) A. Buczek, and T. Telejko, “Investigation of heat transfer coefficient during quenching in various cooling agents,” *Int. J. Heat Fluid Flow*, **44** 358–364 (2013). doi:10.1016/j.ijheatfluidflow.2013.07.004.
- 25) H. Kou, W. Li, X. Zhang, J. Shao, X. Zhang, P. Geng, Y. Deng, and J. Ma, “Effects of mechanical shock on thermal shock behavior of ceramics in quenching experiments,” *Ceram. Int.*, **43** (1) 1584–1587 (2017). doi:10.1016/j.ceramint.2016.10.021.
- 26) Z. LI, M. ZHAN, X. FAN, Y. DONG, and L. XU, “Effect of blank quenching on shear spinning forming precision of 2219 aluminum alloy complex thin-walled components,” *Chinese J. Aeronaut.*, (2023). doi:10.1016/j.cja.2022.11.027.
- 27) P. Mukhopadhyay, “Alloy designation, processing, and use of aa6xxx series aluminium alloys,” *ISRN Metall.*, **2012** (Table 1) 1–15 (2012). doi:10.5402/2012/165082.
- 28) A. Kareem, J.A. Qudeiri, A. Abdudeen, T. Ahammed, and A. Ziout, “A review on aa 6061 metal matrix composites produced by stir casting,” *Materials (Basel)*, **14** (1) 1–22 (2021). doi:10.3390/ma14010175.
- 29) P. Ma, Z.J. Wei, Y.D. Jia, Z.S. Yu, K.G. Prashanth, S.L. Yang, C.G. Li, L.X. Huang, and J. Eckert, “Mechanism of formation of fibrous eutectic si and thermal conductivity of sicp/al-20si composites solidified under high pressure,” *J. Alloys Compd.*, **709** 329–336 (2017). doi:10.1016/j.jallcom.2017.03.162.
- 30) A.K. Sharma, R. Bhandari, A. Aherwar, and C. Pinca-Bretotean, “A study of fabrication methods of aluminum based composites focused on stir casting process,” in: *Mater. Today Proc.*, Elsevier Ltd, 2020:

- pp. 1608–1612. doi:10.1016/j.matpr.2020.03.316.
- 31) S.P. Dwivedi, N.K. Maurya, and M. Maurya, “Assessment of hardness on aa2014/eggshell composite produced via electromagnetic stir casting method,” *Evergreen*, **6** (4) 285–294 (2019). doi:10.5109/2547354.
- 32) H.I. Akbar, E. Surojo, and D. Ariawan, “Investigation of industrial and agro wastes for aluminum matrix composite reinforcement,” *Procedia Struct. Integr.*, **27** (2019) 30–37 (2020). doi:10.1016/j.prostr.2020.07.005.
- 33) X. Wang, Y. Wu, J. Cui, C.Q. Zhu, and X.Z. Wang, “Shape characteristics of coral sand from the south china sea,” *J. Mar. Sci. Eng.*, **8** (10) 1–24 (2020). doi:10.3390/jmse8100803.
- 34) A. V. Sharanova, A.O. Tovpinets, and M.A. Dmitrieva, “Application of sea sand for 3d concrete printing,” *IOP Conf. Ser. Mater. Sci. Eng.*, **597** (1) 1–5 (2019). doi:10.1088/1757-899X/597/1/012033.
- 35) Z. Jalil, A. Rahwanto, Mustanir, Akhyar, and E. Handoko, “Magnetic behavior of natural magnetite (fe<sub>3</sub>o<sub>4</sub>) extracted from beach sand obtained by mechanical alloying method,” *AIP Conf. Proc.*, **1862** (2017). doi:10.1063/1.4991127.
- 36) M.H. Rahman, and H.M.M. Al Rashed, “Characterization of silicon carbide reinforced aluminum matrix composites,” *Procedia Eng.*, **90** 103–109 (2014). doi:10.1016/j.proeng.2014.11.821.
- 37) Japanese Industrial Standard, “JIS Z 2201 : Test Pieces for Tensile Test for Metallic Materials,” in: 2017.
- 38) A.A.S.H. and T.O. Standard, “ASTM E10 : Standard Test Method for Brinell Hardness of Metallic Materials,” in: 2012: pp. 1–32.
- 39) C.H. Gireesh, P.K.G. Durga, and K. Ramji, “Experimental investigation on mechanical properties of an al6061 hybrid metal matrix composite,” *J. Compos. Sci.*, **2** (49) 1–10 (2018). doi:10.3390/jcs2030049.
- 40) V. Garric, K. Colas, P. Donnadieu, G. Renou, and S. Urvoy, “Correlation between quenching rate , mechanical properties and microstructure in thick sections of al-mg-si(-cu) alloys,” *Mater. Sci. Eng. A*, **753** (January) 253–261 (2019). doi:10.1016/j.msea.2019.03.045.
- 41) C. Kannan, and R. Ramanujam, “Comparative study on the mechanical and microstructural characterisation of AA 7075 nano and hybrid nanocomposites produced by stir and squeeze casting,” Cairo University, 2017. doi:10.1016/j.jare.2017.02.005.
- 42) K. Strobel, M.D.H. Lay, M.A. Easton, L. Sweet, S. Zhu, N.C. Parson, and A.J. Hill, “Effects of quench rate and natural ageing on the age hardening behaviour of aluminium alloy aa6060,” *Mater. Charact.*, **111** 43–52 (2016). doi:10.1016/j.matchar.2015.11.009.
- 43) B. Benjunior, A.H. Ahmad, M.M. Rashidi, and M.S. Reza, “Effect of different cooling rates condition on thermal profile and microstructure of aluminium 6061,” *Procedia Eng.*, **184** 298–305 (2017). doi:10.1016/j.proeng.2017.04.098.
- 44) H.Q. Wang, W.L. Sun, and Y.Q. Xing, “Microstructure analysis on 6061 aluminum alloy after casting and diffuses annealing process,” *Phys. Procedia*, **50** (October 2012) 68–75 (2013). doi:10.1016/j.phpro.2013.11.013.
- 45) C.G. Garay-Reyes, L. González-Rodelas, E. Cuadros-Lugo, E. Martínez-Franco, J. Aguilar-Santillan, I. Estrada-Guel, M.C. Maldonado-Orozco, and R. Martínez-Sánchez, “Evaluation of hardness and precipitation in zn-modified al2024alloy after plastic deformation and heat treatments,” *J. Alloys Compd.*, **705** (2017) 1–8 (2017). doi:10.1016/j.jallcom.2017.02.111.
- 46) P.H. Sung, and T.C. Chen, “Effects of quenching rate on crack propagation in nial alloy using molecular dynamics,” *Comput. Mater. Sci.*, **114** 13–17 (2016). doi:10.1016/j.commatsci.2015.11.046.
- 47) P.A. Rometsch, Y. Zhang, and S. Knight, “Heat treatment of 7xxx series aluminium alloys - some recent developments,” *Trans. Nonferrous Met. Soc. China (English Ed.)*, **24** (7) 2003–2017 (2014). doi:10.1016/S1003-6326(14)63306-9.
- 48) G.E. Totten, and A. Clinton, “Handbook of Quenchants and Quenching Technology,” 1993. doi:10.1016/0261-3069(93)90123-d.
- 49) J.S. Robinson, and W. Redington, “The influence of alloy composition on residual stresses in heat treated aluminium alloys,” *Mater. Charact.*, **105** 47–55 (2015). doi:10.1016/j.matchar.2015.04.017.
- 50) X. Chen, L. Zhang, X. Jie, Y. Li, and X. Huang, “Quenching characteristics of glycerol solution as a potential new quenchant,” *Int. J. Heat Mass Transf.*, **109** 209–214 (2017). doi:10.1016/j.ijheatmasstransfer.2017.02.013.
- 51) T. He, H. Li, P. Tang, X. He, and P. Li, “Influence of quenching agent on microstructure, properties and thermal stress of sicp/2009 composites,” *Mater. Charact.*, **118** 547–552 (2016). doi:10.1016/j.matchar.2016.07.002.
- 52) B. Milkereit, and M.J. Starink, “Quench sensitivity of al-mg-si alloys: a model for linear cooling and strengthening,” *Mater. Des.*, **76** 117–129 (2015). doi:10.1016/j.matdes.2015.03.055.
- 53) M.R. Wisnom, M. Gigliotti, N. Ersoy, M. Campbell, and K.D. Potter, “Mechanisms generating residual stresses and distortion during manufacture of polymer-matrix composite structures,” *Compos. Part A Appl. Sci. Manuf.*, **37** (4) 522–529 (2006). doi:10.1016/j.compositesa.2005.05.019.
- 54) S.K. Tiwari, S. Soni, R.S. Rana, and A. Singh, “Effect of heat treatment on mechanical properties of aluminium alloy-fly ash metal matrix composite,” *Mater. Today Proc.*, **4** (2) 3458–3465 (2017). doi:10.1016/j.matpr.2017.02.235.